ISBN: 978-981-18-7950-0
2023 the 13th International Workshop on Computer Science and Engineering (WCSE 2023)
doi: 10.18178/wcse.2023.06.032

Research on Human-Redundant Robot Interaction and Configuration Optimization

Yu Li and Liang Wang +

School of Automation Science and Electrical Engineering, Beihang University, Beijing, China

Abstract. Redundant robots have obvious advantages such as good motion performance, avoiding singularity and joint limit. Human-robot interaction is an important content in robot field. Currently, there are relatively few research on cooperative compliance of redundant robot. Therefore, taking 4-DOF redundant robot as the research object, the forward and inverse kinematics model is obtained. In order to make full use of redundant characteristics, the inverse kinematics algorithm based on augmented Jacobian matrix with the optimization goal of avoiding joint limit is adopted, which greatly shortens the solution time and can meet real-time control requirement. Then, admittance control system is established for human-robot interaction, and force error is converted into motion error. Through the expansion of Jacobian matrix and admittance control system, human-robot interaction is achieved, while configuration optimization control is also realized. The research provides an important reference for compliance interaction of human-redundant robot cooperation.

Keywords: human-robot interaction, redundant robot, admittance control, configuration optimization

1. Introduction

Redundant robots are widely used for its obvious advantages such as good motion performance, avoiding singularity and joint limit [1]. When robots perform complex tasks that require interaction with the environment, it is not only required to meet the motion accuracy requirement, but also to adjust the the contact force. In some complex application environment, human and robot are needed to cooperate to complete the work task. Thus, the compliance control of human-robot contact is an important guarantee to achieve safe, friendly cooperation. It has also become a research hotspot in the robot field [2]. Force control is an important content involved in the research of this field. Force control of robot is to achieve the compliant contact. It mainly includes impedance control, force position hybrid control and other intelligent control methods [3-5]. The ideas contained in these methods have important guiding significance for the research of force control today.

Wang et al. [6] proposed a force/position hybrid control method based on RBF neural network compensation for a rope traction parallel robot support system. Through the dynamic modeling and analysis of the system, the designed force/position hybrid control was substituted into the overall dynamic equation to obtain the error closed-loop system. In addition, Naveen Kumar et al. [7] also conducted the force position hybrid control of 2-DOF constrained reconfigurable manipulator. The neural network adaptive control model based on dynamic model was adopted. The simulation showed that the method has good reliability and robustness. Du et al. [8] studied the human-robot interaction control of tactile main manipulator in laparoscopic minimally invasive surgery robot system. Firstly, a generalized dynamic equation of manipulator was derived based on the momentum. The joint driving torque required by the motion state was tracked. In addition, a compensator based on time-delay neural network was proposed to improve the performance of human-robot interaction. Sadeghian H, et al. [9] studied the control of redundant robots. While controlling the robot in task space, it ensured that the robot has a certain compliant behavior in null space. Based on the dynamic model, the control algorithm was designed, and the force and motion errors were simulated and analyzed.

+ Corresponding author. Tel.: + 86-13001203677.
E-mail address: wangliang@buaa.edu.cn.

In summary, currently, contact interaction control is mainly applied to traditional non-redundant robots. There is relatively less research on redundant robots. As for the redundant robot, it is mainly controlled according to the special self-motion. It does not make full use of redundant characteristics. So configuration optimization can be studied to realize the unification of motion control and interactive control. Compared with traditional robots, redundant robots have significant advantages and are widely used in many fields. Therefore, force control of redundant robots is an important and meaningful research content.

Then, taking the 6-DOF modular robot as the research object, by locking some of its joints, it can be equivalent to a 4-DOF redundant robot that can move in three-dimensional space. For redundant robot, due to the existence of redundant degree of freedom, they have multiple configurations at the same position. At present, the main methods used to solve the inverse problem of redundant robot are generalized inverse method, neural network method, iterative optimization method, etc. These methods have the disadvantages of long calculation time and easy to fall into local optimization [10-11]. Therefore, in this paper, joint limit avoidance is taken as the optimization objective, the optimization model based on the augmented Jacobian matrix is constructed [12], which can improve the speed of solving inverse kinematics of robots and lays an important foundation for effective human-robot cooperation. And the admittance control strategy is proposed to achieve the goal of human-robot interaction and configuration optimization. Finally, the feasibility and effectiveness of the theory are verified through experiment.

2. Kinematics Model

2.1. Robot model

The 6-DOF SCHUNK robot in the laboratory is taken as the research object to conduct relevant research. The 4th and 6th joints are locked and regarded as connecting rods. At this time, the robot becomes a 4-DOF redundant robot, and the redundancy is located on the three-link plane mechanism above the base. The structure of the robot and its mechanism diagram are shown in Figs. 1-2.

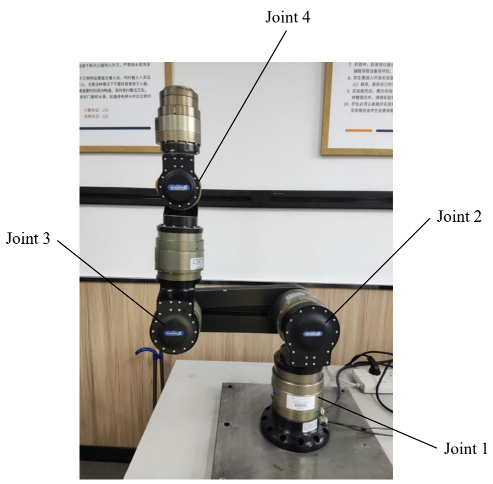

Fig. 1: Structure of SCHUNK robot.

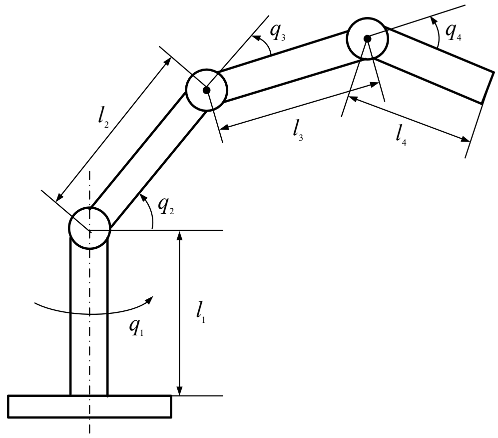

Fig. 2: Mechanism diagram of the robot.

Through measurement, the structural parameters of robot are $l_1 = l_2 = l_3 = 0.3$ m, $l_4 = 0.2$ m.

2.2. Forward kinematics model

The D-H homogeneous matrix transformation method is used to solve the kinematics equation of the robot. According to the robot structure, the D-H parameters of the robot is shown in Table 1.

Table 1: D-H parameters.

i	a_{i-1}	α_{i-1} (°)	d_i	q_i
1	0	0	l_1	q_1
2	0	90	0	q_2
3	l_2	0	0	q_3
4	l_3	0	0	q_4
5	l_4	0	0	0

The transformation matrix between the $i-1$-th and i-th coordinate systems is

$$\begin{aligned} {}^{i-1}_{i}T &= \mathrm{Rot}_x(\alpha_{i-1})\mathrm{Trans}_x(a_{i-1})\mathrm{Rot}_z(q_i)\mathrm{Trans}_z(d_i) \\ &= \begin{bmatrix} \cos q_i & -\sin q_i & 0 & a_{i-1} \\ \sin q_i \cos\alpha_{i-1} & \cos q_i \cos\alpha_{i-1} & -\sin\alpha_{i-1} & -d_i \sin\alpha_{i-1} \\ \sin q_i \sin\alpha_{i-1} & \cos q_i \sin\alpha_{i-1} & \cos\alpha_{i-1} & -d_i \cos\alpha_{i-1} \\ 0 & 0 & 0 & 1 \end{bmatrix} \end{aligned} \tag{1}$$

According to the homogeneous transformation rule, the homogeneous transformation matrix between the end position and the origin is

$${}^{0}_{5}T = {}^{0}_{1}T\,{}^{1}_{2}T\,{}^{2}_{3}T\,{}^{3}_{4}T\,{}^{4}_{5}T \tag{2}$$

Therefore, the position equation of the robot is

$$\begin{cases} x = [l_2 \cos q_2 + l_3 \cos(q_2+q_3) + l_4 \cos(q_2+q_3+q_4)]\cos q_1 \\ y = [l_2 \cos q_2 + l_3 \cos(q_2+q_3) + l_4 \cos(q_2+q_3+q_4)]\sin q_1 \\ z = l_1 + l_2 \sin q_2 + l_3 \sin(q_2+q_3) + l_4 \sin(q_2+q_3+q_4) \end{cases} \tag{3}$$

2.3. Inverse kinematics model

When solving the inverse solution of the robot, the inverse kinematics of the three -link above the base is calculated first. The position of the end of the two-link mechanism is set to (x', y'). By making auxiliary lines along the horizontal and vertical directions at the end points. The distance between the end point and the origin is $S = \sqrt{x'^2 + y'^2}$. Taking S as the hypotenuse, a right triangle is formed. Coordinate diagram of the mechanism is shown in Fig. 3.

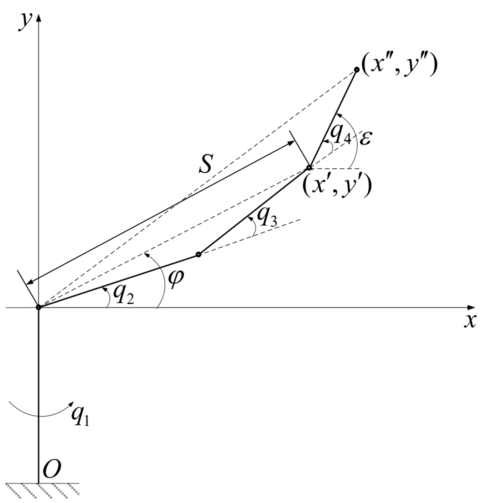

Fig. 3: Coordinate diagram of the mechanism.

The angle passing through the origin is denoted as φ, then there is

$$\varphi = \arctan(\frac{y'}{x'}) \tag{4}$$

$$x' = S\cos\varphi \tag{5}$$

$$y' = S\sin\varphi \tag{6}$$

Then

$$l_3\cos(q_2 + q_3) = x' - l_2\cos(q_2) \tag{7}$$

$$l_3\sin(q_2 + q_3) = y' - l_2\sin(q_2) \tag{8}$$

And $x'^2 + y'^2 = S^2$, combined with the cosine theorem, we can get

$$q_2 = \pm\arccos\left(\frac{x'^2 + y'^2 + l_2^2 - l_3^2}{2Sl_2}\right) + \varphi \tag{9}$$

$$q_3 = \pi - \arccos(\frac{l_2^2 + l_3^2 - x'^2 - y'^2}{2l_2l_3}) \tag{10}$$

The end position of the three-link mechanism above the base is (x'', y''). The angle between the third connecting rod and the horizontal plane is denoted as ε, then

$$\varepsilon = \arctan(\frac{y'' - y'}{x'' - x'}) \tag{11}$$

Since

$$\varepsilon = q_2 + q_3 + q_4 \tag{12}$$

So the third joint angle of three-link mechanism is

$$q_4 = \varepsilon - q_2 - q_3 \tag{13}$$

When the base rotates q_1 angle, it forms a three-dimensional motion space. At this moment, the end position is recorded as (x, y, z). The solution expression of rotation angle is as follows.

$$q_1 = \arctan(\frac{y}{x}) \tag{14}$$

In the three-dimensional space, the coordinate form used in the previous inverse solution of the planar three-link mechanism is changed. Projecting the coordinates of three-dimensional space to a plane, there are

$$x'' = \sqrt{x^2 + y^2} \ \ (\text{or } x'' = \frac{x}{\cos q_1}\ ) \tag{15}$$

$$y'' = z - l_1 \tag{16}$$

$$x' = x'' - l_4\cos\varepsilon \tag{17}$$

$$y' = y'' - l_4\sin\varepsilon \tag{18}$$

The above is inverse kinematics model of 4-DOF redundant robot. While meeting the primary goal in given task space, the configuration of robot can be adjusted to achieve secondary goal.

3. Optimization Model Based on Augmented Jacobian Matrix

As for inverse kinematics model in the previous chapter, it needs to sample the redundant parameter ε first. However, it takes a long time to solve this algorithm in practical application. Then, the inverse kinematics algorithm of redundant robot is proposed based on augmented Jacobian matrix. The inverse kinematics of the robot is expressed as an optimization problem.

$$\begin{cases} \min W(q) \\ s.t.F(q)=0 \end{cases} \tag{19}$$

where $F(q)=f(q)-P$, P is the target position, $f(q)$ is the forward kinematics, and $W(q)$ is the target function to be optimized. Define the Lagrange function

$$L(q,\mu)=W(q)+\mu^{\mathrm{T}}F(q) \tag{20}$$

where μ is the Lagrange factor. When the objective function takes the extreme value, there should be

$$\frac{\partial L(q,\mu)}{\partial q}=\frac{\partial W(q)}{\partial q}+\mu^{\mathrm{T}}\frac{\partial F(q)}{\partial q}=0 \tag{21}$$

where $\frac{\partial F(q)}{\partial q}$ is the Jacobian matrix $J(q)$ of the robot. Equation (21) can be written as

$$\frac{\partial L(q,\mu)}{\partial q}=\frac{\partial W(q)}{\partial q}+\mu^{\mathrm{T}}J(q)=0 \tag{22}$$

The null space of the robot is $N=I-J^{+}J$, then the extended motion constraint is

$$Z=N\frac{\partial W}{\partial q} \tag{23}$$

Equation (23) is taken as an additional constraint of the kinematics, the expanded differential kinematics can be written as

$$\begin{bmatrix} \dot{P} \\ \dot{Z} \end{bmatrix}=J_a(q)\dot{q} \tag{24}$$

In Equation (24), $J_a(q)$ is the augmented Jacobian matrix, which is expressed as

$$J_a(q)=\begin{bmatrix} J \\ J_N \end{bmatrix} \tag{25}$$

where $J_N=\frac{\partial}{\partial q}(N\frac{\partial W}{\partial q})$, then the joint velocity can be expressed as

$$\dot{q}=J_a^{-1}(q)\begin{bmatrix} \dot{P} \\ \dot{Z} \end{bmatrix} \tag{26}$$

Due to structure of some joints themself, they can only move within a certain range. Here, the joint avoidance limit criterion is selected as the objective function to evaluate the distance between the current joint angle and the joint center. The function is projected to the null space of the Jacobian matrix to optimize the joint motion and avoid the joint limit as far as possible [13]. It is defined as

$$W(q)=\sum_{i=1}^{n}\frac{1}{4}\frac{(q_{i\max}-q_{i\min})^2}{(q_{i\max}-q_i)(q_i-q_{i\min})} \tag{27}$$

In Equation (27), $q_{i\max}$ and $q_{i\min}$ are the upper and lower limits of the i-th joint q_i, respectively. And the upper and lower limits of joint angle are $q_1,q_4\in[-\pi,\pi]$ and $q_2,q_3\in[-\pi/2,\pi/2]$. The gradient vector $\nabla W(q)$ of the optimization index $W(q)$ is used to replace the free vector in Equation (23) to obtain the joint avoidance limit optimization equation. The gradient vector is

$$\nabla W(q) = \left[\frac{\partial W}{\partial q_1}, \frac{\partial W}{\partial q_2}, \cdots \frac{\partial W}{\partial q_n} \right]^{\mathrm{T}} \tag{28}$$

And

$$\frac{\partial W}{\partial q_i} = \frac{(q_{i\max} - q_{i\min})^2 (2q_i - q_{i\max} - q_{i\min})}{4(q_{i\max} - q_i)^2 (q_i - q_{i\min})^2} \tag{29}$$

By using the above optimization model, the robot can avoid the limit of joints as much as possible and maintain a good configuration.

4. Admittance Control Model

Because the robot is a nonlinear, highly coupled system, it is difficult to obtain the precise parameters of the dynamic model. So this paper adopts position-based impedance control, namely, admittance control. The model of the robot in contact with the environment is shown in Fig. 4.

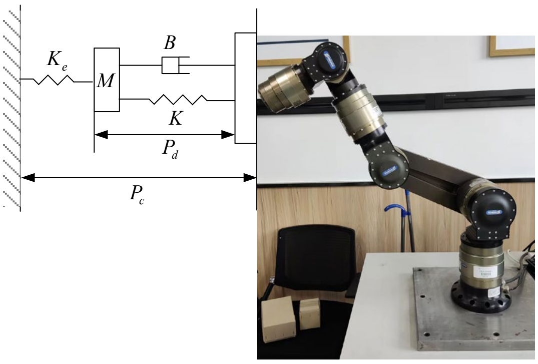

Fig. 4: Contact model between robot and environment.

According to the relationship between the position of the robot end and the force, the impedance model can be expressed as follows.

$$M(P_c - P_d)'' + B(P_c - P_d)' + K(P_c - P_d) = \Delta F \tag{30}$$

$$M\ddot{E} + B\dot{E} + KE = \Delta F \tag{31}$$

Wherein, $E = P_c - P_d$ is tracking error, and $\Delta F = F_e - F_d$ is the force tracking error.

Under the background of dragging teaching, the desired force $F_d = 0$, and the reference trajectory is fixed point, i.e., $P_d = 0$. The control strategy can be considered as $M = 0$, $K = 0$. Since $V_c = \dot{P}_c$, then, taking Laplace transform on both ends of Equation (31), the transfer function can be obtained as follows.

$$G(s) = \frac{V_c(s)}{\Delta F(s)} = \frac{1}{B} \tag{32}$$

In fact, the external force F_e is related to the position of the robot. K_a is the expected admittance value. The speed control signal V_c in Cartesian space is obtained through PID controller. The velocity control signal in joint space is obtained through the inverse J_a^{-1} of the augmented Jacobian matrix. In the experiment, the control law needs to be written in the discrete form. The difference $\Delta P = P_c(k) - P_c(k-1)$ between the target position and the current position should be used. According to

$$\Delta q = J_a^{-1}(q) \begin{bmatrix} \Delta P \\ 0 \end{bmatrix} \tag{33}$$

The target joint angle is calculated as follows.

$$q_c(k) = q_c(k-1) + \Delta q \tag{34}$$

Thus, the admittance control of the robot is completed.

In the experiment of human-robot cooperative control, the direct way is to use a force sensor, which is installed on the end effector of the robot and gives real-time feedback. The control formula is as follows.

$$\Delta P = K_a F \tag{35}$$

F represents the force signal collected by force sensor, ΔP represents the increment of position. K_a is the admittance coefficient. It reflects the motion value of the robot caused by the dragging external force, which can also be called the external force transmission coefficient. The bigger K_a is, the lighter human feels, and the easier robot is to drag. The force is converted into the position increment, which is sent periodically as a control variable, and then the dragging teaching can be realized without any dynamic model or gravity compensation of robot.

5. Experiment

Based on the proposed method, the program is compiled and the dragging experiment is carried out to verify the safety and friendliness of human-robot interaction. The three-dimensional force sensor of LA3D46 series is used. The force control project of the robot is built in Visual Studio. Then the serial port program of the force sensor is added, so that the data of force sensor can be read and adjusted in real time. Finally, combining with the admittance control algorithm, human-robot cooperation can be realized.

For admittance control system, the Cartesian space can be decomposed into three independent controls in the actual programming, and the integrator can be realized by summation. The admittance coefficient $K_a = 0.8$. PID parameters $K_p = 1$, $K_I = 0$, $K_D = 1.5$, respectively, namely PD control, which can effectively improve the dynamic performance. The sampling period $T = 1$ ms, and the baud rate of force sensor communication is 9600. The experimental results are shown in Figs. 5-6.

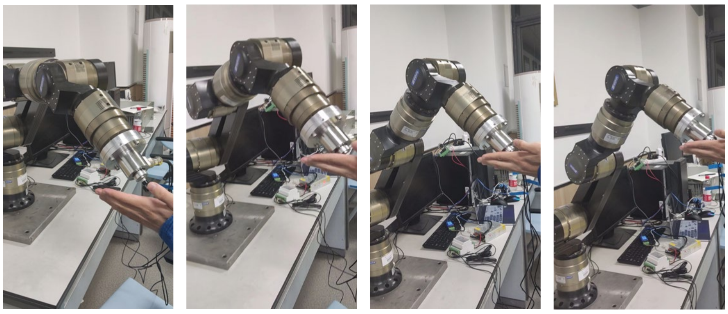

Fig. 5: Compliant dragging process of robot.

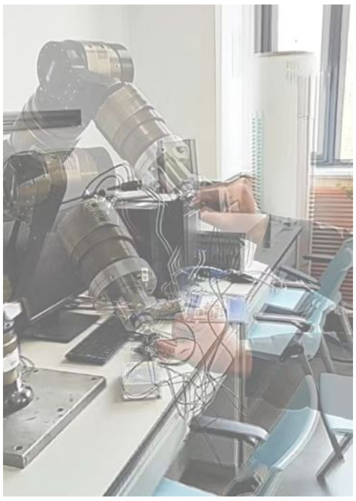

Fig. 6: Dynamic diagram of human-robot interaction.

The experiment shows that the manipulator can move along the direction of external force with good compliance. The degree of compliance can be adjusted by adjusting the compliant coefficient K_a, and the parameters of PID controller can be adjusted to make the manipulator have better motion performance. Based on the configuration optimization model, the robot can maintain a good configuration while achieving force control.The result shows that the control method is feasible and effective. Besides, this method avoids the difficulty of obtaining dynamic models and selecting reference trajectory.

6. Conclusions

Taking 4-DOF redundant robot as the research object, this paper studies the interaction problem of human-redundant robot, with emphasis on the analysis of compliant dragging. Configuration optimization and human-robot interaction are realized, so that redundant degree of freedom is fully utilized. D-H method and geometric projection method are used to establish the kinematics model of the robot. The optimization model based on augmented Jacobian matrix is established with the goal of avoiding the joint limit, which greatly improves the solution speed of inverse kinematics. In addition, the admittance control system of redundant robot is established. The experimental results show that the proposed control method can realize compliance of human-robot interaction and enable the robot to maintain a good configuration, which is of great significance for application of redundant robot and friendly human-robot cooperation.

7. References

[1] Shimizu M, Kakuya H, Yoon W K, et al. Analytical Inverse Kinematic Computation for 7-DOF Redundant Manipulators With Joint Limits and Its Application to Redundancy Resolution. *IEEE Transactions on Robotics*, 2008, 24(5):1131-1142.

[2] Mojtaba, Sharifi, Saeed, et al. Model reference adaptive impedance control in Cartesian coordinates for physical human–robot interaction. *Advanced Robotics*, 2014, 28(19):1277-1290.

[3] Geravand M, Flacco F, AD Luca. Human-robot physical interaction and collaboration using an industrial robot with a closed control architecture. *IEEE International Conference on Robotics & Automation*, 2013, 3985–3992.

[4] Hogan N. Impedance Control: An Approach to Manipulation, Part I-Theory, Part II-Implementation, Part III-Application. *ASME Journal of Dynamic System, Measurement and Control*, 1985,107(1):1-24.

[5] Raibert M H, Craig J J. Hybrid position/force control of manipulators. *ASME Journal of Dynamic Systems, Measurement and Control*, 1981, 102(2):126-133.

[6] Wang Yuqi, Lin Qi, Wang Xiaoguang, et al. Force/position hybrid control of a rope traction parallel robot support system based on RBF neural network compensation. *Control and Decision*, 2020, 35(03): 536-546.

[7] Kumar N, Rani M. Neural network-based hybrid force/position control of constrained reconfigurable manipulators. *Neurocomputing*, 2021, 420(3):1-14.

[8] Zhijiang Du, Yunlei Lianga, Zhiyuan Yan, et al. Human-robot interaction control of a haptic master manipulator used in laparoscopic minimally invasive surgical robot system. *Mechanism and Machine Theory*, 2021, 156, 104132.

[9] Sadeghian, H, Villani, et al. Task-Space Control of Robot Manipulators With Null-Space Compliance. *IEEE Transactions on Robotics*, 2014, 30(2):493–506.

[10] Taghirad H.D., Bedoustani, Y.B. An Analytic-Iterative Redundancy Resolution Scheme for Cable-Driven Redundant Parallel Manipulators. *IEEE Transactions on Robotics*, 2011, 27(6):1137–1143.

[11] Cui Z, Tang X, Hou S, et al. Non-iterative geometric method for cable-tension optimization of cable-driven parallel robots with 2 redundant cables. *Mechatronics*, 2019, 59:49–60.

[12] Pyung, Chang. A closed-form solution for inverse kinematics of robot manipulators with redundancy. *IEEE Journal on Robotics and Automation*, 1987, 3(5):393–403.

[13] Dubey R V, Euler J A, Babcock S M. Real-Time Implementation of an Optimization Scheme for Seven-Degree-of-Freedom Redundant Manipulators. *IEEE Transactions on Robotics and Automation*, 1991, 7(5):579-588.